Table 1 is a tabulation of the optimal location of the actuator for the noncollocated and collocated cases. Because all of the controllers were designed to generate identical dynamics, the control power is used as a corroborator of the use of the weighted cost functions for determining the optimal location of the actuator. Table 1 lists the optimal locations of the actuators and the normalized control power. It can be seen that weighting the cost function with the component cost results in a significant reduction of the control power as in J_3 and J_4, J_5 and J_6, and J_7 and J_8. Note that J_1, J_2, J_6, and J_8 result in requiring nearly identical control power.

V. Conclusions

In this Note, a methodology for determining the optimal actuator and sensor locations for the control of combustion instabilities is presented. The approach relies on the quantitative measures of the degree of controllability and component cost. These criteria are arrived at by considering the energies of system's inputs and outputs. The optimality criteria for sensor and actuator locations provide a balance between the importance of the lower-order (controlled) and the higher- (residual) order modes.

In previous studies, the cost has been a function of the control influence matrix only and the relative contribution of the modes to the output has not been considered. This Note describes a systematic procedure that associates weights that reflect the importance of each state variable or mode in a given cost function, thus, increasing the system controllability and its overall performance. The procedure can be extended to optimize the number of actuators in multi-input applications by removing the least effective actuators, one at a time. In addition, it can be applied to a discrete set of candidate locations. The control energy level can be taken as a factor in the selection process, in a sense that if the head/end location is not practical, the optimal location can be moved to the next control energy level and so on. In general, the optimal locations are found to be at locations where the lower modes have the greatest contribution and the higher modes are minimally represented in the cost functions. Physically speaking, at these locations, the lower modes are the most controllable because the point of application of the actuation power is far from the nodal point of these modes, which means the required control is small and the higher modes are not excited.

References

[1]Skelton, R., and Yousuff, A., "Component Cost Analysis of Large Scale Systems," *International Journal of Control*, Vol. 137, No. 2, 1983, pp. 285–304.

[2]Hamdan, A., and Nayfeh, A., "Measure of Modal Controllability and Observability for First- and Second-Order Linear Systems," *Journal of Guidance, Control, and Dynamics*, Vol. 12, No. 5, 1989, pp. 421–428.

[3]Junkins, J., and Kim, Y., *Introduction to Dynamics and Control of Flexible Structures*, AIAA, Washington, DC, 1993.

[4]Longman, R. W., and Alfriend, K. T., "Energy Optimal Degree of Controllability and Observability for Regulator and Maneuver Problems," *Journal of the Astronautical Sciences*, Vol. 38, 1990, pp. 87–103.

[5]Lim, K., "Method for Optimal Actuator and Sensor Placement for Large Flexible Structure," *Journal of Guidance, Control, and Dynamics*, Vol. 15, No. 1, 1992, pp. 49–57.

[6]Fung, Y.-T., Yang, V., and Sinha, A., "Active Control of Combustion of Instabilities with Distributed Actuators," *Combustion Science and Technology*, Vol. 78, 1991, pp. 217–245.

[7]Fung, Y.-T., Yang, V., and Sinha, A., "State-Feedback Control of Longitudinal Combustion Instabilities," *Journal of Propulsion and Power*, Vol. 8, No. 1, 1992, pp. 66–75.

[8]Choe, K., and Baruh, H., "Actuator Placement in Structural Control," *Journal of Guidance, Control, and Dynamics*, Vol. 15, No. 1, 1992, pp. 40–48.

Modified Mixing Analogy for Studies of Mixing in Supersonic Flows

Sadatake Tomioka*
National Aerospace Laboratory of Japan, Kakuda, Miyagi 981-1525, Japan
and
Lance S. Jacobsen† and Joseph A. Schetz‡
Virginia Polytechnic Institute and State University, Blacksburg, Virginia 24061-0203

Nomenclature

M	=	Mach number
P, p	=	total and static pressure
q	=	dynamic pressure
T	=	total temperature
V	=	velocity
α	=	injectant mass fraction
α_{mix}	=	injectant mass fraction deduced with modified mixing analogy, Eq. (3)
α^*_{mix}	=	injectant mass fraction deduced with original mixing analogy, Eq. (1)
β	=	enthalpy deficit factor due to induced vorticity
ρ	=	density

Subscripts

a	=	freestream
c	=	unheated injection
h	=	heated injection
j	=	injectant
p	=	measured with in-stream probe

Introduction

MIXING augmentation techniques[1–4] are an essential requirement for the development of the supersonic combustion ramjet (scramjet) engine. In recent works,[3,5] a high-molecular-weight injectant was utilized because hydrocarbon fuels became of greater interest.[6–8] However, many injectant concentration detection techniques depend mainly on the difference between the injectant molecular weight and that of the main flow so that their sensitivity is not sufficient compared to cases with lighter molecules, for example, helium, injected into air. In some previous work,[3] therefore, heated air was injected into an unheated supersonic crossflow, and the corresponding equivalent injectant concentration was deduced from the total temperature measurements and a mixing analogy as

$$\alpha^*_{\text{mix}} = (T_p - T_a)/(T_j - T_a) \tag{1}$$

Received 30 March 2001; revision received 20 May 2002; accepted for publication 12 September 2002.

*Senior Researcher, Ramjet Propulsion Center, Kakuda Space Propulsion Laboratory. Member AIAA.

†Graduate Assistant, Aerospace and Ocean Engineering Department; currently, Postdoctoral Research Engineer, U.S. Air Force Research Laboratory, Dayton, OH 45433-7251. Member AIAA.

‡Fred D. Durham Chair, Aerospace and Ocean Engineering Department. Fellow AIAA.

in which a turbulent Lewis number of unity was assumed. A similar technique has also been utilized to study jet mixing[9] and the mixing of a jet and a subsonic crossflow.[10] However, in cases with heated air injection into a supersonic crossflow, vorticity effects shown by the Crocco theorem were found to change the enthalpy field, and negative equivalent injectant concentration was deduced in some regions through the original mixing analogy (see Ref. 3). Because heated air injection combined with the temperature measurements is inexpensive and safe, modification of the mixing analogy to isolate the vorticity effects from the mixing data would be useful for studies on high-speed mixing phenomena.

In the present study, we propose a modified mixing analogy to deduce concentration from a measured total temperature with vorticity effects taken into account. This method was tested for the injection through a diamond-shaped orifice oriented perpendicular to a Mach 3 supersonic airflow. Both heated and unheated air were injected with sonic speed, and total temperature distributions were measured in the mixing flowfield. The vorticity effects were canceled out by comparing the results with heated and unheated injection, and the corresponding injectant concentration was deduced. To evaluate the validity of the new mixing analogy, the injectant concentration was measured directly with an aspirating-type concentration probe by introducing a small amount of tracer helium into the injectant air.

Modified Mixing Analogy

For our modified mixing analogy, we conducted both heated ($T_a \sim 380$ K) and unheated ($T_a \sim 285$ K) air injection. When it is assumed that 1) the local injectant equivalent concentration α is insensitive to the injectant temperature and 2) the effects of the induced vorticity on the change in local enthalpy are proportional through a factor β to the local enthalpy, and the proportionality is insensitive to the injectant temperature, the enthalpy balances for the heated and unheated cases can be written as

$$(T_p)_h = (1-\beta)[(1-\alpha)(T_a)_h + \alpha(T_j)_h] \tag{2a}$$

$$(T_p)_c = (1-\beta)[(1-\alpha)(T_a)_c + \alpha(T_j)_c] \tag{2b}$$

From Eq. (2), a modified expression for the deduced injectant mass fraction was derived as

$$\alpha_{\text{mix}} = [(T_p/T_a)_h/(T_p/T_a)_c - 1]/\{(T_p/T_a)_h/(T_p/T_a)_c \times [1-(T_j/T_a)_c] - [1-(T_j/T_a)_h]\} \tag{3}$$

This is to be compared to the earlier expression in Eq. (1). Both T_j and T_p were normalized with simultaneously measured T_a to eliminate the effects of any T_a variation (typically decreased by 6 K in a 10-s run) on the data reduction. From Eqs. (2) and (3), we can obtain

$$\beta = 1 - (T_p/T_a)_h/[(1-\alpha_{\text{mix}}) + \alpha_{\text{mix}}(T_j/T_a)_h] \tag{4}$$

The modified mixing analogy method requires identical local values of both α_{mix} and β in the heated and unheated injection cases, whereas the difference in injectant temperature resulted in a slight difference in governing parameters of injection and mixing (summarized in Table 1) even at an identical dynamic pressure ratio. (In this study, $q_j/q_a = 2.0$.) As regards the identical α assumption, Chrans and Collins[11] showed that total temperature of the jet had little effect on the initial penetration (Mach disk) height. Billig et al.[12] also showed that the jet trajectories were well described by the momentum equation, so that the difference in jet temperature would not affect the trajectory of a sonic jet issued into supersonic flow. Kamotani and Greber[10] reported that the jet trajectories are mainly determined by the dynamic pressure ratio in the case with a perpendicular jet injected into a subsonic crossflow. For coaxial jet mixing, Zakkay et al.[13] showed that the maximum concentration decays, and the concentration profiles with various injectant are well correlated with mass flux ratio, also shown in Table 1. In the present case, the difference in mass flux ratio due to the injectant temperature difference was 14%, and we expect only minor effects of it on the mixing process. Thus, one could expect almost identical equivalent injectant distributions in the heated and unheated cases. However, Bowersox et al.[14] reported effects of injectant temperature on the flow properties in the lower half of the mixing layer, close to the wall, with two-dimensional slot injection into a supersonic flow, and so we should be careful of data reduction near the wall.

As for the validation of the identical β assumption, we only could verify the similarity in flowfields, regardless of the injectant temperature. Figure 1 shows a comparison of the Mach number distribution on the symmetry plane with both heated and unheated injections. The distributions agree well with each other, showing that the flowfields were almost identical, regardless of injectant temperature over the range studied here.

Table 1 Dominant parameters with various injectant and/or conditions

Injectant	Heated air	Air + 15%He	Unheated air
V_j/V_a	0.588	0.548	0.509
ρ_j/ρ_a	57.9	66.7	77.1
$(\rho V)_j/(\rho V)_a$	34.0	36.6	39.2
p_j/p_a	18	17.7	18

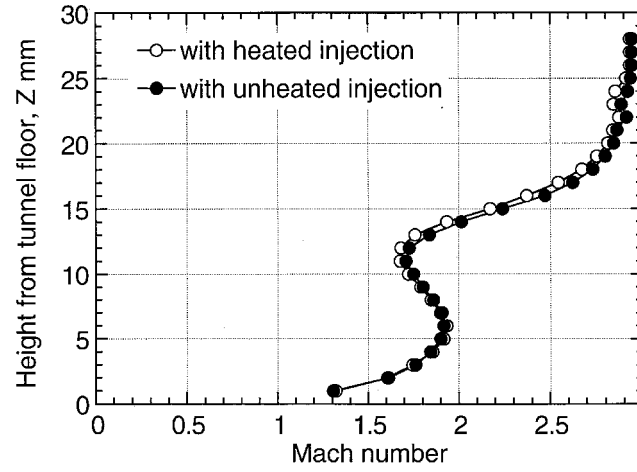

Fig. 1 Mach number distributions on contour symmetry plane at 110 mm downstream of the injector center.

Validation of the Modified Mixing Analogy

Experimental Methods

The facility is of a blowdown type, with a half-nozzle to accelerate the airflow to Mach 3. The tunnel average plenum conditions were 620 kPa (P_a) and 285 K (T_a), which resulted in a freestream Reynolds number of 5.0×10^7/m. The boundary-layer thickness and displacement thickness at the injector location were 8.5 and 3.3 mm, respectively.

The diamond-shaped orifice used in the present study had a half-angle of 10 deg on both its leading and trailing edges, and an equivalent diameter of 4.1 mm. The discharge coefficient was measured to be 0.85. Air was used as the injectant to simulate a high-molecular-weight gas hydrocarbon fuel injection. A portion of the air was bypassed from the tunnel plenum chamber to the injectant plenum chamber and injected with sonic speed at the jet-to-freestream dynamic pressure ratio q_j/q_a of $2.0 \pm 5\%$. The injectant air could be heated to about 380 K with two electric heaters in the injector plenum chamber.

Pressures (P_a and P_j) and temperatures (T_a and T_j) within the plenum chambers were monitored. The flow was probed in a plane 110 mm downstream from the center of the injector by a pitot probe (a 1.59/1.04 mm o.d./i.d. tube), cone static probe (a 1.59-mm o.d. tube with a 10-deg cone half-angle), a total temperature probe (see Ref. 3 for detailed description of probe), and a concentration measurement probe.

The total temperature measurements of the freestream resulted in a total temperature recovery factor of 0.98 and a temperature

measurement error of ±2 K. The true total temperature was evaluated from the measured total temperature, measured Mach number, and a recovery factor of 0.98.

Two aspirating hot-film probes[2,15,16] were used to measure the in-stream helium concentration and to monitor the injectant helium concentration when a tracer was used. The in-stream probe was designed to assure shock swallowing at its tip, and it had a tip hole diameter of 0.64 mm. A commercially available hot film was installed within the probe inner tube (3.86-mm i.d.). The aspirated gas was exhausted into a vacuum tank through a small internal orifice (0.64-mm i.d.). Pressure and temperature within the probe and the bridge voltage of a hot-film anemometer (IFA 100) were monitored.

The probe was calibrated by aspirating air/helium mixtures with known concentrations and pressures in a vessel. (See Ref. 16 for details). The typical error of the concentration measurement was ±1% of the mole fraction of the helium; however, the error increased for in-probe Reynolds numbers of 6×10^2–9×10^2, where the internal flow in the probe caused separation leading to larger errors.

For the direct measurement, the helium concentration of the unheated mixture was kept as low as 15/vol% to make the governing injection parameters close to those in the air injection cases, as shown in Table 1.

Results

Figure 2 shows the measured and deduced injectant mass fraction distributions along the contour symmetry plane. An equivalent mass fraction distribution obtained with the original mixing analogy [Eq. (1)] is shown with open circular symbols, the equivalent mass fraction distribution obtained with the modified mixing analogy [Eq. (3)] is shown with open square symbols, and the directly measured mass fraction with an He tracer is shown with solid circular symbols. Error bars for the measured injectant mass fraction data are also shown. This error appears exaggerated in Fig. 2 because the injectant contained only 15/vol% helium. Despite the large scatter and error, the directly measured injectant mass concentration distribution showed a similar trend to the equivalent mass fraction distribution obtained with the modified mixing analogy, and it showed rather good agreement near the plume core. Thus, the plume penetration height and maximum injectant concentration are well documented with the injectant concentrations deduced from the modified mixing analogy. Note that nonphysical negative values of equivalent mass fraction were mostly avoided with the modified mixing analogy.

The discrepancy between the measured and deduced injectant concentrations were larger in the vicinity of the wall, which was expected from Ref. 14. Thus, one must be careful when interpreting data in regions very near to the wall through the modified analogy.

The injectant mass fraction distribution deduced with the modified mixing analogy based on the measured total temperature without correction due to the probe temperature recovery factor are also shown in Fig. 2 with X symbols. It is almost identical to the distribution based on the corrected total temperature.

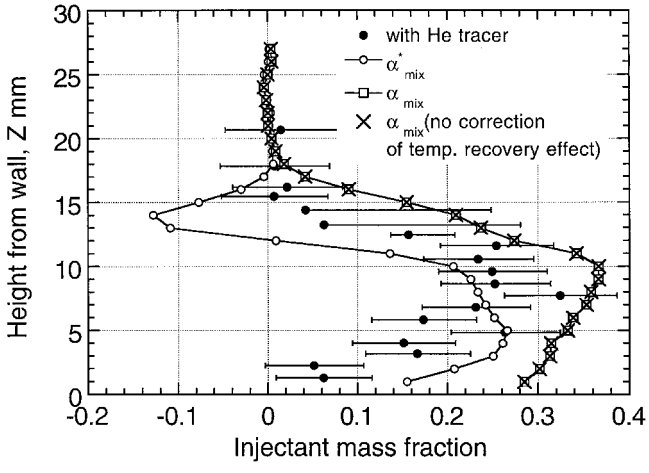

Fig. 2 Injectant mass fraction distributions on contour symmetry plane at 110 mm downstream of the injector center.

Table 2 Estimation of error on α_{mix} due to temperature measurement errors

Variable	Temperature, K	$d\alpha_{mix}$, +2 K	$d\alpha_{mix}$, −2 K
$(T_a)_h$	285.0	−0.018	0.017
$(T_j)_h$	360.7	−0.010	0.010
$(T_p)_h$	298.4	0.029	−0.029
$(T_a)_c$	285.0	0.018	−0.020
$(T_j)_c$	287.3	0.011	−0.011
$(T_p)_c$	272.7	−0.031	0.032

Another validation method used was to integrate the injectant mass flux to obtain the injectant mass flow rate and to compare that with the injected flow rate measured with the orifice flowmeter. The local flow state was calculated based on the corrected total temperature and the measured pitot and cone static pressures. The calculated equivalent mass flow rate with the original mixing analogy was 14% less than the injected mass flow rate, whereas that with the modified mixing analogy was 8% less than the injected mass flow rate, indicating better results with the modified mixing analogy.

Error Estimation of the Modified Analogy

As noted earlier, we expect temperature measurement errors of ±2 K. Table 2 shows estimated error in equivalent mass fraction based on a typical set of measured temperature data and the expected temperature measurement errors. The error in equivalent mass fraction was estimated to be ±3% at most.

Conclusions

The conventional mixing analogy was based on "turbulent Le = 1" assumption, which resulted in large errors in the deduced injectant concentration due to vorticity effects on the enthalpy field in high-speed mixing studies. The mixing analogy was modified in the present study to take the vorticity effects into account, and deduced concentration data were evaluated against direct measurements of injectant concentration with a tracer technique for the trial case of the interaction of a heated-air jet from a diamond-shaped, sonic injector orifice and a Mach 3 supersonic air-flow. The resulting deduced injectant concentration distribution showed good agreement with that measured by the helium tracing technique. The tracer technique itself was subject to rather large uncertainties resulting from the requirement of keeping the initial fraction of the tracer low (15% by volume) in order to allow matching of the injection parameters. Error estimation was done to show that ±3% error on injectant mass fraction was expected for a nominal ±2 K measurement error on temperature in the present measurement technique. The modified mixing analogy presented here should prove very useful in future high-speed mixing studies. We plan to employ it in such work and to continue validation and refinement of the method.

References

[1]Schetz, J. A., Thomas, R. H., and Billig, F. S., "Mixing of Transverse Jets and Wall Jets in Supersonic Flow," *Separated Flows and Jets*, edited by V. V. Kozlov and A. V. Dovgal, Springer-Verlag, Berlin, 1991, pp. 807–837.

[2]Fuller, R. P., Wu, P.-K., Nejad, A. S., and Schetz, J. A. , "Comparison of Physical and Aerodynamic Ramps as Fuel Injectors in Supersonic Flow," *Journal of Propulsion and Power*, Vol. 14, No. 2, 1998, pp. 135–145.

[3]Jacobsen, L. S., Schetz, J. A., and Ng, W. F., "Flowfield Near a Multiport Injector Array in a Supersonic Flow," *Journal of Propulsion and Power*, Vol. 16, No. 2, 2000, pp. 216–226.

[4]Barber, M. J., Schetz, J. A., and Roe, L. A., "Normal, Sonic Helium Injection Through a Wedge-Shaped Orifice into Supersonic Flow," *Journal of Propulsion and Power*, Vol. 13, No. 2, 1997, pp. 257–263.

[5]Gruber, M. R., Nejad, A. S., Chen, T. H., and Dutton, J. C., "Mixing and Penetration Studies of Sonic Jets in a Mach 2 Freestream," *Journal of Propulsion and Power*, Vol. 11, No. 2, 1995, pp. 315–323.

[6]Mathur, T., Streby, G., Gruber, M, Jackson, K., Donbar, J., Donaldson, W., Jackson, T., Smith, C., and Billig, F., "Supersonic Combustion Experiments with a Cavity-Based Fuel Injector," AIAA Paper 99-2102,

1999; also *Journal of Propulsion and Power*, Vol. 17, No. 6, 2001, pp. 1305–1312.

[7]Vinogradov, V. A., Kobigsky, S. A., and Petrov, M. D., "Experimental Investigation of Kerosene Fuel Combustion in Supersonic Flow," *Journal of Propulsion and Power*, Vol. 11, No. 1, 1995, pp. 130–134.

[8]Morrison, C. Q., Campbell, R. L., Edelman, R. B., and Jaul, W. K., "Hydrocarbon Fueled Dual-Mode Ramjet/Scramjet Concept Evaluation," International Symposium on Air Breathing Engines, Paper 97-7053, Sept. 1997.

[9]Schadow, K. C., Gutmark, E., Koshigoe, S., and Wilson, K. J., "Combustion-Related Shear-Flow Dynamics in Elliptic Supersonic Jets," *AIAA Journal*, Vol. 27, No. 10, 1989, pp. 1347–1353.

[10]Kamotani, Y., and Greber, I., "Experiments on a Turbulent Jet in a Crossflow," *AIAA Journal*, Vol. 10, No. 11, 1972, pp. 1425–1429.

[11]Chrans, L. J., and Collins, D. J., "Stagnation Temperature and Molecular Weight Effects in Jet Interaction," *AIAA Journal*, Vol. 8, No. 2, 1970, pp. 287–293.

[12]Billig, F. S., Orth, R. C., and Lasky, M., "Unified Analysis of Gaseous Jet Penetration," *AIAA Journal*, Vol. 9, No. 6, 1971, pp. 1048–1058.

[13]Zakkay, V., Krause, E., and Woo, S. D. L., "Turbulent Transport Properties for Axisymmetric Heterogeneous Mixing," *AIAA Journal*, Vol. 2, No. 11, 1964, pp. 1939–1947.

[14]Bowersox, R. D. W., Tucker, K. C., and Whitcomb, C. D., "Two-Dimensional Nonadiabatic Injection into a Supersonic Freestream," *Journal of Propulsion and Power*, Vol. 16, No. 2, 1995, pp. 234–242.

[15]Ninnemann, T. A., and Ng, W. F., "A Concentration Probe for the Study of Mixing in Supersonic Shear Flows," *Experiments in Fluids*, Vol. 13, 1992, pp. 98–104.

[16]Xillo, O. C., Schetz, J. A., and Ng, W. F., "A Sampling Probe for Fluctuating Concentration Measurements in Supersonic Flow," AIAA Paper 99-0519, Jan. 1999.